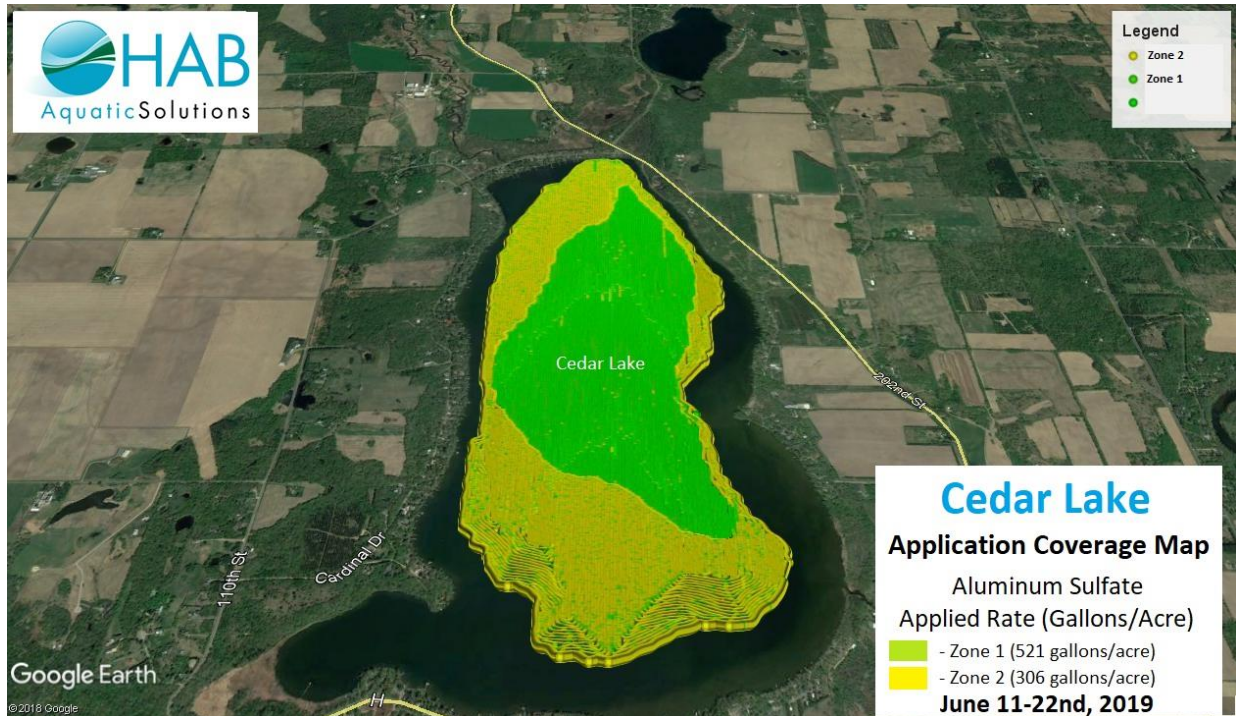


# Cedar Lake, Wisconsin - Limnological response to alum treatment: 2019 interim report



Aerial map of alum application to Cedar Lake in 2019. Credits: HAB Aquatic Solutions, St. Paul, MN

15 November, 2019



University of Wisconsin – Stout  
Sustainability Sciences Institute - Center for  
Limnological Research and Rehabilitation  
Department of Biology  
123E Jarvis Hall  
Menomonie, Wisconsin 54751  
715-338-4395  
[jamesw@uwstout.edu](mailto:jamesw@uwstout.edu)

Harmony  
Environmental

Finding a balance

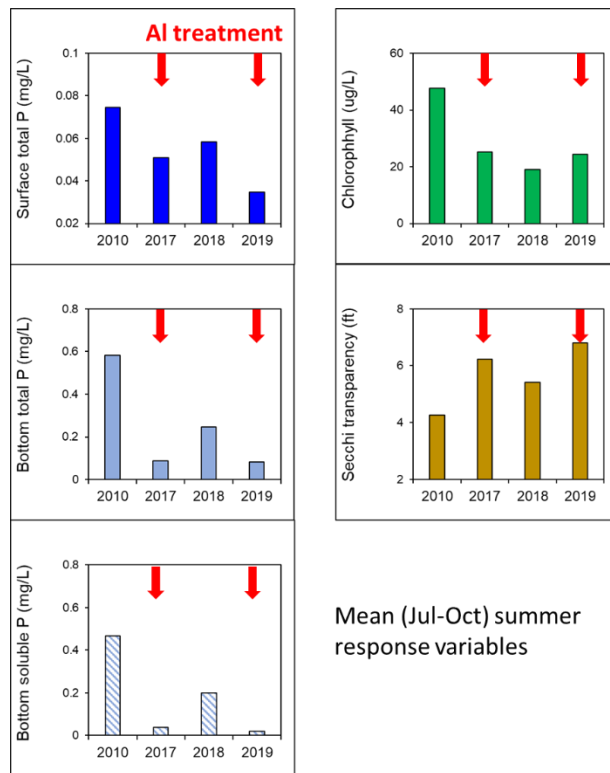


People Land Water

Harmony Environmental  
516 Keller Ave S  
Amery, Wisconsin 54001  
715-268-9992  
[harmonyenv@amerytel.net](mailto:harmonyenv@amerytel.net)

## Executive Summary

- Approximately 22 g/m<sup>2</sup> and 28 g/m<sup>2</sup> alum (i.e., aluminum sulfate) were applied to sediment located between the 20-25 ft and > 25 ft contours, respectively, between 11-22 June 2019. This treatment represented ~ 22% of the total concentration and was the second in a series of alum applications to the lake that will be conducted over ~ 10 y.
- Post-Al treatment mean summer (Jul-early Oct) concentrations of surface total phosphorus (P) and chlorophyll were lower in 2019 compared to pretreatment conditions. In particular, mean summer chlorophyll was 24 µg/L in 2019, representing a 49% improvement over the 2010 summer mean of 48 µg/L.
- A modest algal bloom developed in September 2019 after the Al application, similar to patterns observed after the 2017 Al treatment. This unusual phenomenon may reflect exploitation of P-limited conditions by an otherwise rarely observed algal species in Cedar Lake that has a resting stage (i.e., akinetes or cysts) and stored surplus cellular P prior to the 2019 Al application. This unusual pattern seems to be temporary and likely will not occur again in 2020.
- Bottom total P and soluble reactive P (SRP) concentrations were very low throughout the 2019 summer season, suggesting substantial control of internal P loading as a result of the second alum treatment. Net internal P loading in 2019, determined by P mass balance, was reduced by essentially ~ 100% relative to 2010 (-177 kg v 3,723 kg, respectively). Laboratory-derived diffusive P flux under anaerobic conditions declined by 85% in 2019 (2.3 mg/m<sup>2</sup> d) compared to mean rates measured in 2010 (15 mg/m<sup>2</sup> d).



## Objectives

Multiple Al applications over a period of 10-12 years are planned for Cedar Lake in order to control internal phosphorus loading. It is critical to conduct post-treatment monitoring of water and sediment chemistry to document the trajectory of water quality improvement during rehabilitation to make informed decisions regarding adjusting management to meet future water quality goals. Post-treatment monitoring included field and laboratory research to document changes in 1) hydrology and watershed phosphorus (P) loading, 2) the P budget and lake water quality, 3) binding of sediment mobile P fractions that have contributed to internal P loading by alum, and 4) rates of diffusive P flux from the sediment under anaerobic conditions. Overall, lake water quality is predicted to respond to watershed and internal P loading reduction with lower surface concentrations of total P and chlorophyll concentrations throughout the summer, lower bloom frequency of nuisance chlorophyll levels, and higher water transparency. Multiple Al applications between 2017 and 2029 should result in the binding of iron-bound P and substantial reduction in diffusive P flux from sediments under anaerobic conditions (i.e., internal P loading). The first alum application occurred in late June 2017. The Al concentration was 20 g/m<sup>2</sup> for sediment located within the 20-25 ft depth contour and 26 g/m<sup>2</sup> for sediment located at depths > 25 ft. The second alum application occurred during 11-22 June 2019 and Al concentrations ranged between 22 g/m<sup>2</sup> within the 20-25 ft depth contour and ~ 28 g/m<sup>2</sup> for depths > 25 ft. Current combined Al application of 42 g/m<sup>2</sup> and 54 g/m<sup>2</sup> to the two depth zones represents ~ 42% of the target Al doses of 100 g/m<sup>2</sup> and 130 g/m<sup>2</sup>. The objectives of this interim report were to describe the 2019 limnological and sediment variable response to these alum treatments in Cedar Lake. Limnological monitoring is being used in conjunction with an adaptive management approach to gauge lake response and the need, if any, to adjust Al dose or application strategy.

## Methods

### *Alum application in 2019*

Alum (aluminum sulfate) was applied to Cedar Lake by HAB Aquatic Solutions (St. Paul, MN) between 11 and 22 June 2019. The Al dosage was 22 g/m<sup>2</sup> (306 gal/ac) between the 20-25 ft

depth contours and 28 g/m<sup>2</sup> (521 gallons/ac, see cover photo).

### *Watershed loading and lake monitoring*

A gauging station was established on Horse Creek above Cedar Lake at 10<sup>th</sup> Ave for concentration, loading, and flow determination between May and October 2019 (Fig. 1). Grab samples were collected biweekly at the 10<sup>th</sup> Ave gauging station for chemical analysis. Water samples were analyzed for TSS, total P, and soluble reactive P (SRP) using standard methods (APHA 2011, Wisconsin State Lab of Hygiene). Summer tributary P loading was calculated using the computer program FLUX.

The deep basin water quality station WQ 2 was sampled biweekly between May and October 2019 (Fig. 1). An integrated sample over the upper 2-m was collected for analysis of total P, SRP, and chlorophyll a. An additional discrete sample was collected within 0.5 m of the sediment surface for analysis of total and SRP. Secchi transparency and in situ measurements (temperature, dissolved oxygen, pH, and conductivity) were collected on each date using a YSI 6600 sonde (Yellow Springs Instruments) that was calibrated against dissolved oxygen Winkler titrations (APHA 2011) and known buffer solutions.

### *Sediment chemistry*

*Sediment characteristics.* A sediment core was collected in August and late September 2019 at WQ 2 (Fig. 1) for determination of vertical profiles of various sediment characteristics and phosphorus fractions (see Analytical methods below). The sediment core was sectioned at 1-cm intervals between 0 and 10 cm and at 2-cm intervals below the 10-cm depth for determination of moisture content, wet and dry bulk density, loss-on-ignition organic matter, loosely-bound P, iron-bound P, labile organic P, and aluminum-bound P.

### *Laboratory-derived diffusive phosphorus flux from sediments under anaerobic conditions.*

Anaerobic diffusive P fluxes were measured from intact sediment cores collected at stations shown in Figure 1 in August 2019. One sediment core was collected at each station to monitor

alum treatment effectiveness after application. The sediment incubation systems were placed in a darkened environmental chamber and incubated at 20 °C for up to 5 days. The incubation temperature was set to a standard temperature for all stations for comparative purposes. The oxidation-reduction environment in each system was controlled by gently bubbling nitrogen through an air stone placed just above the sediment surface to maintain anaerobic conditions.

Water samples for SRP were collected from the center of each system using an acid-washed syringe and filtered through a 0.45 µm membrane syringe filter (Nalge). The water volume removed from each system during sampling was replaced by addition of filtered lake water preadjusted to the proper oxidation-reduction condition. These volumes were accurately measured for determination of dilution effects. Rates of P release from the sediment (mg/m<sup>2</sup> d) were calculated as the linear change in mass in the overlying water divided by time (days) and the area (m<sup>2</sup>) of the incubation core liner. Regression analysis was used to estimate rates over the linear portion of the data.

*Analytical methods.* A known volume of sediment was dried at 105 °C for determination of moisture content, wet and dry bulk density, and burned at 550 °C for determination of loss-on-ignition organic matter content (Avnimelech et al. 2001, Håkanson and Jansson 2002). Phosphorus fractionation was conducted according to Hietjes and Lijklema (1980), Psenner and Puckso (1988), and Nürnberg (1988) for the determination of ammonium-chloride-extractable P (loosely-bound P), bicarbonate-dithionite-extractable P (i.e., iron-bound P), and sodium hydroxide-extractable P (i.e., aluminum-bound P).

The loosely-bound and iron-bound P fractions are readily mobilized at the sediment-water interface as a result of anaerobic conditions that lead to desorption of P from sediment and diffusion into the overlying water column (Mortimer 1971, Boström et al. 1982, Boström 1984, Nürnberg 1988). The sum of the loosely-bound and iron-bound P fraction represents redox-sensitive P (i.e., the P fraction that is active in P release under anaerobic and reducing conditions) and will be referred to as *redox-P*. Aluminum-bound P reflects P bound to the Al floc after aluminum sulfate application and its chemical transformation to aluminum hydroxide (Al(OH)<sub>3</sub>).

## Summary of Results

### *Hydrology and phosphorus loading*

On an annual basis, precipitation in 2019 was above average at ~43 inches compared to the ~ 33-inch average since 1980 (Fig. 2). Monthly precipitation exceeded the long-term average for most months (Fig. 3). In contrast, monthly precipitation was much less than the long-term average in July 2019.

Horse Creek summer flow exhibited major peaks between April and May 2019 in conjunction with spring storms (Fig. 4). Flows subsided during a period of low precipitation in June, then increased as a result of storms in early July. Flows also peaked in early September and October. Horse Creek mean summer (May-October) daily flow was relatively high at 0.57 m<sup>3</sup>/s in 2019 (Fig. 5), reflecting greater precipitation, and comparable to 2010 and 2017 mean flows.

Total P concentrations in Horse Creek were elevated between May and mid-July 2019 (Fig. 6). Elevated total P coincided, in part, with higher inflows between May and mid-June; however, total P remained high in early to mid-July despite declines in flow (Fig. 6). Soluble reactive P concentrations also increased to a maximum during this lower flow period. Reasons for this pattern are not precisely known but might be related to unidentified events occurring in upstream portions of the watershed (Horse Lake and Big Lake discharges). In addition, some of the total P input may not have been associated with precipitation-related runoff. Concentrations of both constituents declined during the lower flow period of mid-August through September.

Concentration-flow relationships in 2019 were generally similar to those observed historically (Fig. 7). Flow-averaged summer (May through October) total P and SRP in 2019 were 0.083 mg/L and 0.035 mg/L, respectively, slightly lower than averages estimated for 2018 (Table 1). The flow-averaged SRP concentration accounted for ~42% of the total P in 2019. Summer total P and SRP loadings from Horse Creek were 4.07 and 1.72 kg/d (Table 1), respectively, in 2019, similar to loads estimates during research in 2009-11 and 2017.

Table 1. Mean summer (May-October) constituent concentrations and loading for the Horse Creek inflow station at 10th Ave.

Year	Variable	TSS	Total P	SRP
2010	Concentration (mg/L)		0.089	0.031
	Load (kg/d)		4.18	1.42
2017	Concentration (mg/L)	15.2	0.084	0.034
	Load (kg/d)	767.8	4.26	1.71
2018	Concentration (mg/L)	16.5	0.100	0.039
	Load (kg/d)	549	3.36	1.28
2019	Concentration (mg/L)	10.6	0.083	0.035
	Load (kg/d)	524	4.07	1.72

*Lake limnological response*

Cedar Lake was stratified between late-May and late-August 2019 (Fig. 8). Complete water column mixing and turnover occurred in early-September 2019. Bottom water anoxia was established between early June and late-August 2019. Anoxia extended to about 6.0 m in 2019 compared to ~ 5.5 m in 2010. This pattern may have been related to reduced algal productivity, resulting in less organic carbon deposition to fuel sediment dissolved oxygen demand. Alum application in mid-June 2019 occurred during a period of stable stratification and established hypolimnetic anoxia.

Prior to the 2019 alum treatment, total P and SRP concentrations increased in the bottom waters in conjunction with the development of hypolimnetic anoxia in early June, suggesting the beginning of internal P loading (Fig. 9). Bottom water P concentrations declined as a result of the June 2019 alum treatment and remained low and nominal throughout the summer. Unlike 2018 when hypolimnetic P concentrations increased near the sediment-water interface in August (Fig. 9), the 2019 alum treatment completely controlled hypolimnetic P and concentrations were low above the sediment-water interface throughout the summer (Fig. 10).

Surface total P was relatively low throughout the summer of 2019 in conjunction with the alum application (Fig. 9) Surface total P concentrations increased gradually to a peak of only 0.042 mg/L in late September (Fig 9). In addition, total P concentrations were uniformly low throughout the upper 5 m water column throughout the summer of 2019 (Fig. 10).

Surface chlorophyll concentrations increased to a modest peak of  $\sim 20 \mu\text{g/L}$  in early June before the 2019 alum application (Fig 11). Concentrations declined and were relatively low ( $< 20 \mu\text{g/L}$ ) between July and August 2019, after the alum application, ranging between  $13 \mu\text{g/L}$  and  $17 \mu\text{g/L}$  (Fig. 11). However, chlorophyll exhibited a modest seasonal increase in concentration between mid-August and late September, similar to patterns observed after the 2017 alum treatment (Fig. 11). Although concentrations were still lower in Fall of 2019 compared to pretreatment levels observed in 2010, they increased to a peak of  $\sim 42 \mu\text{g/L}$  on 1 October 2019 (Fig. 11), and algal chlorophyll was distributed throughout the water column as a result of Fall turnover (Fig. 10). Strong winds during this period also concentrated algae toward the shoreline, resulting in scum formation and eventual decomposition with associated odor problems.

By comparison, chlorophyll also increased to  $\sim 40 \mu\text{g/L}$  in early September 2017 (Fig. 10 and 11). However, this fall 2017 bloom was dominated by *Ceratium hirundinella* (not cyanobacteria), which otherwise occurred infrequently and was a rare part of the Cedar Lake species assemblage in 2009-2011. Since *C. hirundinella* forms dormant resting cysts that reside in the sediment, it may have had a competitive advantage and exploited an otherwise empty niche after the 2017 alum treatment. While other algal species became severely P-limited after the alum treatment, *C. hirundinella* cysts probably stored surplus cellular P prior to the treatment that was used for growth during inoculation of the water column. Blooms of otherwise rarely seen algal species, specific because they have a resting stage in the sediment as part of their life cycle, have been observed after alum application in other lakes as well. Because akinetes, cysts, or other resting stages can store surplus P in their cells for longer periods, they can form blooms by using that stored P for growth rather than relying of available P in the water column.

The typical seasonal chlorophyll pattern in years prior to alum treatment saw a substantial

increase in concentration during Fall turnover due to entrainment of hypolimnetic SRP and uptake by cyanobacteria (James et al. 2015). For instance, in 2010 chlorophyll increased from ~ 22  $\mu\text{g/L}$  in mid-July to a maximum ~ 110  $\mu\text{g/L}$  in early October (Fig. 11). Unlike Fall patterns in 2017 through 2019, chlorophyll concentrations remained high and maximal for extended periods (i.e., September through early November) during Fall turnover as in 2010.

Secchi transparency remained improved in conjunction with alum treatment in 2019 (Fig. 12). Prior to alum treatment, as in 2010, Secchi transparency was often unusually high in June, exceeding 2 to 3 m (James 2014, 2015). Transparency declined to a minimum ( $< 1.0$  m) during periods of extended cyanobacteria blooms driven by Fall turnover and hypolimnetic SRP entrainment (Fig. 12, 2010). In 2019, Secchi transparency was very high in May, exceeding 8 ft. It declined to ~ 5 ft in early June, then increased to ~ 9 ft in July as a result of the 2019 alum treatment (Fig. 12). Secchi transparency declined between August and October 2019, but still exceeded 4 to 6 ft. On a seasonal basis, Secchi transparency was much improved compared to the pretreatment year of 2010 (Fig. 12).

Secchi transparency exhibited a significant inverse pattern to that of chlorophyll, indicating that light extinction was due to algae versus inorganic turbidity (Fig. 13). Thus, lower chlorophyll concentrations translated into higher Secchi transparency, particularly during the Fall of 2017 through 2019.

A comparison of mean summer (July-early October) limnological response variables before alum treatment (i.e., 2010) versus 2019 is shown in Figure 14 and Table 2. Mean bottom total P and SRP declined substantially in 2019 in response to the second alum treatment (Fig. 14), and were ~ 86% and 96% lower, respectively, compared to pretreatment 2010 means (Table 2). Mean summer surface total P declined to 0.035 mg/L, falling below the mean target concentration of 0.040 mg/L (Table 2). Mean chlorophyll was higher (24  $\mu\text{g/L}$ ) in 2019 due to the anomalous bloom but the mean was, nevertheless, 49% lower than the pretreatment mean. Finally, mean

Secchi transparency improved to 6.8 ft (Fig. 14 and Table 2).

Variable		2010	2017	2018	2019	Percent improvement over 2010 means			Goal after internal P loading control	
						2017	2018	2019		
Lake	Mean (Jul-Oct)	Mean surface TP (mg/L)	0.074	0.051	0.058	0.035	31% reduction	22% reduction	53% reduction	< 0.040
		Mean bottom TP (mg/L)	0.583	0.088	0.246	0.082	85% reduction	58% reduction	86% reduction	< 0.050
		Mean bottom SRP (mg/L)	0.467	0.038	0.199	0.02	92% reduction	57% reduction	96% reduction	< 0.050
		Mean chlorophyll (ug/L)	47.63	25.17	19.08	24.31	47% reduction	60% reduction	49% reduction	< 15
		Mean Secchi transparency (ft)	4.27	6.28	5.41	6.81	46% increase	27% increase	59% reduction	12.1
	Early Fall peak (i.e. late August-early October)	Surface TP (mg/L)	0.130	0.081	0.115	0.042	38% reduction	11% reduction	68% reduction	NA
		Bottom TP (mg/L)	1.216	0.13	0.543	0.206	89% reduction	55% reduction	83% reduction	NA
		Bottom SRP (mg/L)	1.092	0.068	0.468	0.092	94% reduction	57% reduction	92% reduction	NA
		Chlorophyll (ug/L)	109.6	42.95	27.63	42.00	61% reduction	75% reduction	62% reduction	NA
		Secchi transparency (ft)	2.66	3.61	3.63	3.94	36% increase	37% increase	48% reduction	NA
Sediment	Net internal P loading (kg/summer)	3,723	1,150	1,062	-177	69% reduction	71% reduction	100% reduction	< 400	
	Net internal P loading (mg/m <sup>2</sup> d)	8.8	3.2	2.8	-0.5	64% reduction	66% reduction	100% reduction	< 1.5	
	Sediment diffusive P flux (mg/m <sup>2</sup> d)	15.01	9.53	10.66	2.31	37% reduction	29% reduction	85% reduction	< 1.5	
	Redox-P (mg/g)	0.457	0.276	0.331	ND	37% reduction	28% reduction		< 0.100	
	Al-bound P (mg/g)	0.097	0.160	0.175	ND	65% increase	80% increase		NA	

Cedar Lake P mass exhibited negligible seasonal increases in 2019 (Fig. 15). Peak lake P mass was only 1,080 kg in 2019 compared to a maximum of > 4,000 kg in 2010. As indicated in James (2014, 2015), summer P mass increases were due almost entirely to internal P loading from anoxic sediment prior to alum treatment. Net internal P loading was substantial in 2010 at 3,723 kg (Table 3). In contrast, net internal P loading was negligible in 2019 as a result of the second alum treatment (Table 3). Thus, the 2019 net internal P loading rate represented a 100% reduction over the rate estimated for the summer of 2010. When normalized with respect to the time period used in the estimation of net internal P loading (kg/d), the rate was essentially 0 kg/d versus 2010, representing a 100% improvement over the 2010 rate of 38 kg/d (Table 3).

Summer	Period (d)	$P_{tributary}$ (kg)	$P_{discharge}$ (kg)	$P_{retention}$ (kg)	$P_{lake\ storage}$ (kg)	$P_{net\ int\ load}$ (kg)	$P_{net\ int\ load}$ (kg/d)	$P_{net\ int\ load}$ (mg/m <sup>2</sup> d)
2010	97	445	238	207	3,931	<b>3,723</b>	<b>38</b>	<b>8.8</b>
2017	83	349	212	137	1,287	<b>1,150</b>	<b>14</b>	<b>3.2</b>
2018	87	279	122	157	1,227	<b>1,062</b>	<b>12</b>	<b>3.0</b>
2019	85	346	141	205	28	<b>-77</b>	<b>-1</b>	<b>0</b>

The pattern of seasonal P mass increase in the epilimnion versus the hypolimnion also changed in conjunction with the 2019 alum treatment (Fig. 16). For instance, the anoxic hypolimnion accounted for most of the seasonal P mass increase in 2010 (Fig. 16). By comparison, hypolimnetic P mass accumulation was minor in 2019, indicating nearly complete suppression of net internal P loading from anoxic sediment (Fig. 16).

### *Changes in sediment chemistry and anaerobic diffusive phosphorus flux*

Laboratory-derived anaerobic diffusive P fluxes declined substantially at all stations in August 2019 in response to the June 2019 alum treatment (Fig. 17). Indeed, anaerobic diffusive P fluxes approached zero at many stations in the lake, suggesting complete suppression by the 2019 alum treatment (Fig. 17). When all stations were considered, anaerobic diffusive P flux decreased by a mean 85% versus 2010 pretreatment fluxes (mean rate =  $2.31 \text{ mg/m}^2 \text{ d} \pm 0.38 \text{ SE}$  in 2019; Table 3).

Vertically in the sediment column at station WQ 2 concentrations of iron-bound P were lower in the upper 5 cm sediment layer in 2019 relative to June 2017 (Fig. 18). Since redox-P is related to anaerobic diffusive P flux and, therefore, plays an important role in internal P loading (Nürnberg 1988, Pilgrim et al. 2007), lower redox-P concentrations in 2019 reflected continued internal P loading control in Cedar Lake. In contrast, aluminum-bound P concentrations were elevated in the upper 5-cm layer in 2019, suggesting continued binding of P by the Al floc (Fig. 18).

## **Summary and recommendations**

Mean summer (Jul-Oct) surface total P improved to below target goals in 2019 as a result of alum treatment and was 53% lower than the 2010 pretreatment mean (Table 2). The mean summer chlorophyll concentration remained lower in 2019 at  $24 \text{ } \mu\text{g/L}$ , representing a 49% improvement versus the pretreatment year 2010 ( $48 \text{ } \mu\text{g/L}$ ). However, mean summer chlorophyll concentration was influenced by a modest bloom that developed in late August through

September. I suspect this post Al treatment algal bloom was the result of an otherwise rarely observed algal species that stored surplus cellular P while in a resting stage in the sediment prior to the application. As in 2017, this species exploited the empty niche resulting from severe P limitation of growth of other algal species during the 2019 treatment year. Unfortunately, strong winds moved the algal bloom to the shoreline areas, causing nuisance scums and odor problems. I predict these issues will subside in 2020.

Hypolimnetic post-alum treatment P remained low during the summer of 2019 throughout the summer (Table 2). Net internal P loading in 2019, determined by P mass balance, was reduced by essentially ~ 100% relative to 2010. The 2019 post-treatment laboratory-derived mean diffusive P flux was also ~ 85% lower compared to the 2010 mean.

The next Al application should tentatively be scheduled for 2022. The goal with lower dose alum treatments are to 1) spread costs for alum out over a longer time period and into smaller cost increments and 2) increase overall Al binding efficiency and binding capacity by exposing lower Al doses to sediment and hypolimnetic P. Monitoring and adaptive management approaches are being used to assess water quality and sediment response in order to adjust application timing and Al dosage if necessary to meet goals and expectations.

## References

APHA (American Public Health Association). 2011. Standard Methods for the Examination of Water and Wastewater. 22th ed. American Public Health Association, American Water Works Association, Water Environment Federation.

Avnimelech Y, Ritvo G, Meijer LE, Kochba M. 2001. Water content, organic carbon and dry bulk density in flooded sediments. *Aquacult Eng* 25:25-33.

de Vicente I, Huang P, Andersen FØ, Jensen HS. 2008. Phosphate adsorption by fresh and aged aluminum hydroxide. Consequences for lake restoration. *Environ Sci Technol* 42:6650-6655.

Håkanson L, Jansson M. 2002. Principles of lake sedimentology. The Blackburn Press, Caldwell, NJ USA.

Hjieltjes AH, Lijklema L. 1980. Fractionation of inorganic phosphorus in calcareous sediments. *J Environ Qual* 8: 130-132.

James WF. 2012. Limnological and aquatic macrophyte biomass characteristics in Half Moon Lake, Eau Claire, Wisconsin, 2012: Interim letter report. University of Wisconsin – Stout, Sustainability Sciences Institute – Discovery Center, Menomonie, WI.

James WF. 2014. Phosphorus budget and management strategies for Cedar Lake, WI. University of Wisconsin – Stout, Sustainability Sciences Institute – Discovery Center, Menomonie, WI.

James WF. 2017. Phosphorus binding dynamics in the aluminum floc layer of Half Moon Lake, Wisconsin. *Lake Reserv Manage* 33:130-142.

James WF, PW Sorge, PJ Garrison. 2015. Managing internal phosphorus loading in a weakly stratified eutrophic lake. *Lake Reserv Manage* 31:292-305.

Mortimer CH. 1971. Chemical exchanges between sediments and water in the Great Lakes – Speculations on probable regulatory mechanisms. *Limnol Oceanogr* 16:387-404.

Nürnberg GK. 1988. Prediction of phosphorus release rates from total and reductant-soluble phosphorus in anoxic lake sediments. *Can J Fish Aquat Sci* 45:453-462.

Nürnberg GK. 2009. Assessing internal phosphorus load – Problems to be solved. *Lake Reserv Manage* 25:419-432.

Pilgrim KM, Huser BJ, Brezonik PL. 2007. A method for comparative evaluation of whole-lake and inflow alum treatment. *Wat Res.* 41:1215-1224.

Psenner R, Puckso R. 1988. Phosphorus fractionation: Advantages and limits of the method for the study of sediment P origins and interactions. *Arch Hydrobiol Biel Erg Limnol* 30:43-59.

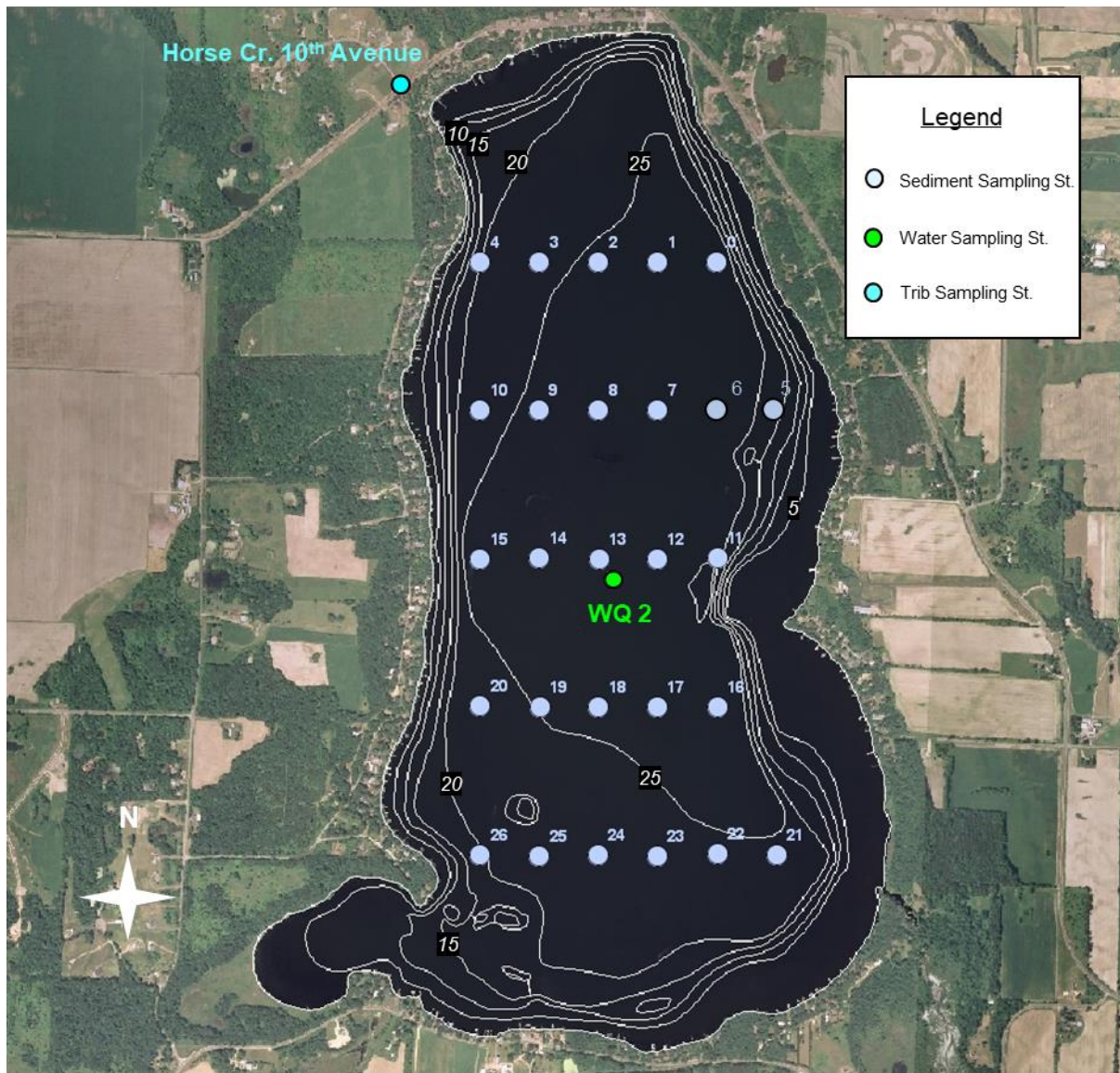


Figure 1. Sediment and water sampling stations.

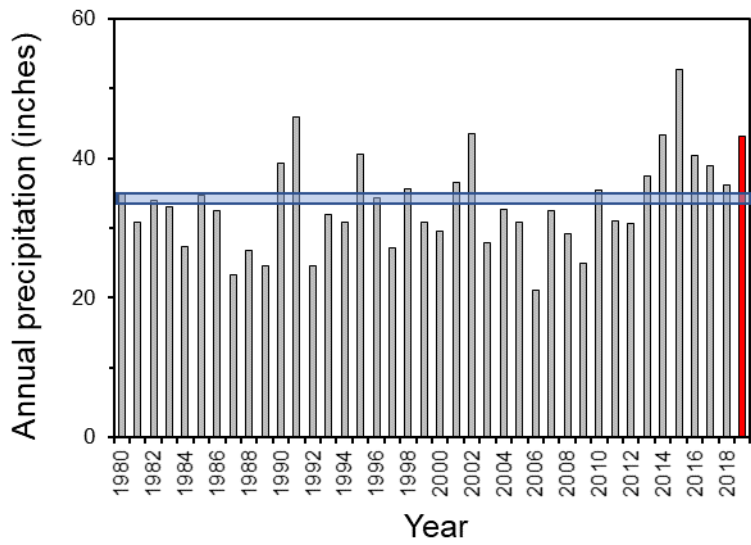


Figure 2. Variations in annual precipitation at Amery, WI. Blue horizontal line represents the average. The year 2019 is highlighted in red.

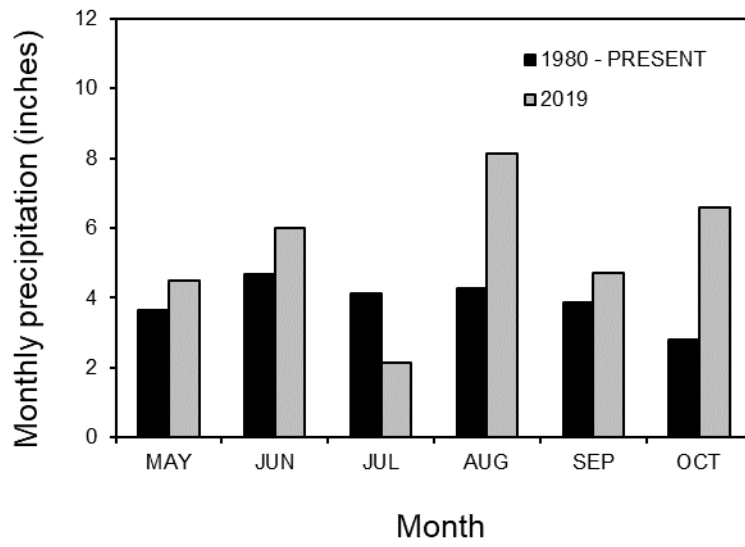


Figure 3. A comparison of average monthly precipitation.

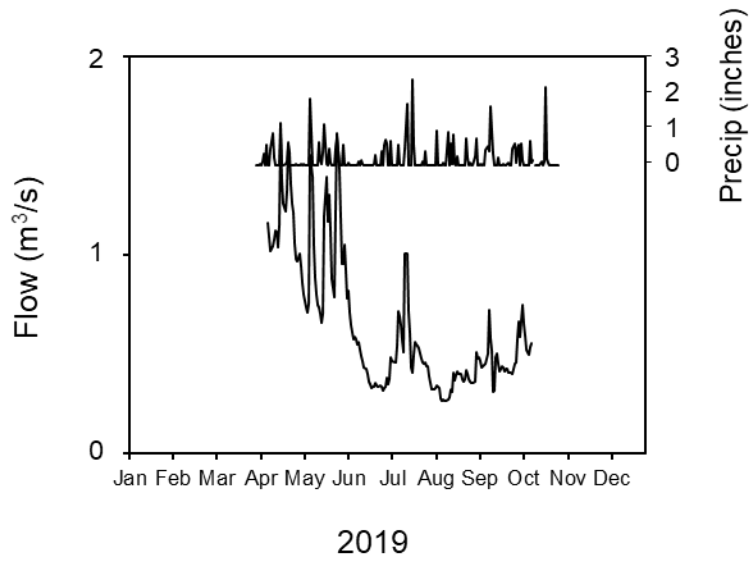


Figure 4. Seasonal variations in daily precipitation at Amery, WI, and flow for Horse Creek at 10<sup>th</sup> Ave.

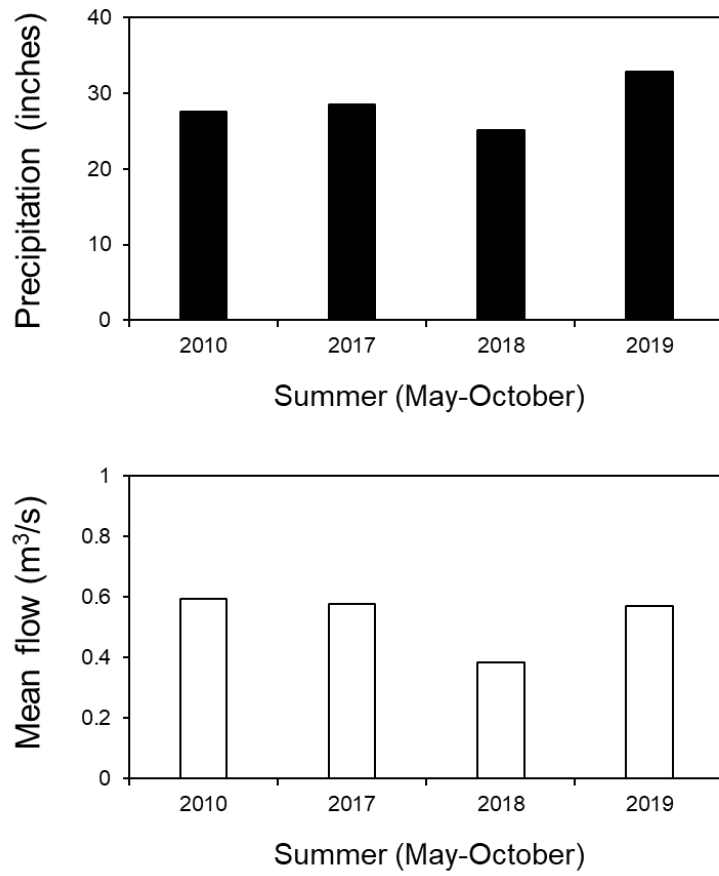


Figure 5. A comparison of summer (May-October) precipitation (upper panel) and mean Horse Creek flow (lower panel). The summer of 2010 was a pretreatment year. Alum was applied to the lake in late June 2017 and 2019.

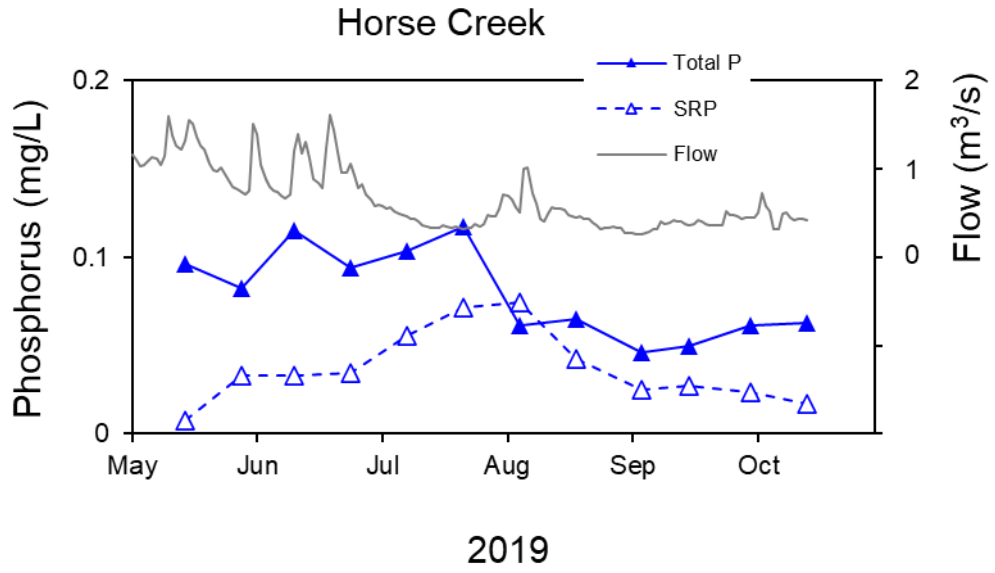


Figure 6. Seasonal variations in total phosphorus (P) and soluble reactive P (SRP) concentration at Horse Creek.

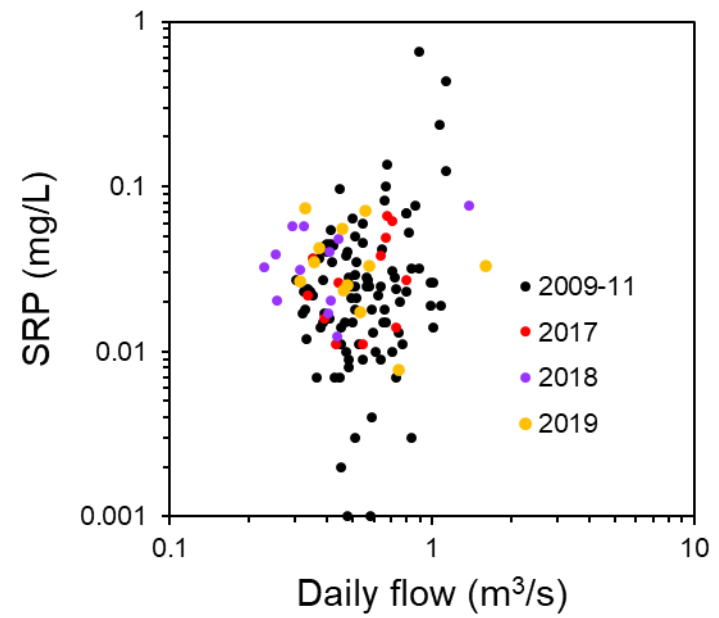
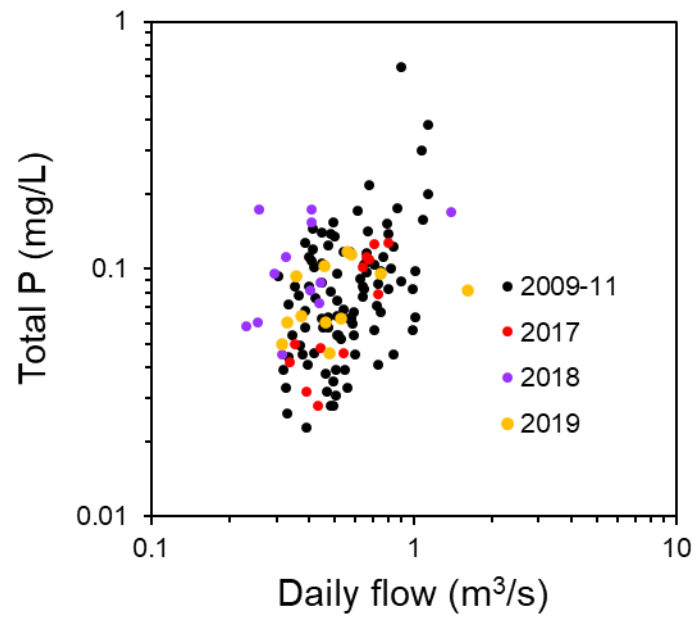


Figure 7. Phosphorus (P) concentration versus daily flow at Horse Creek.

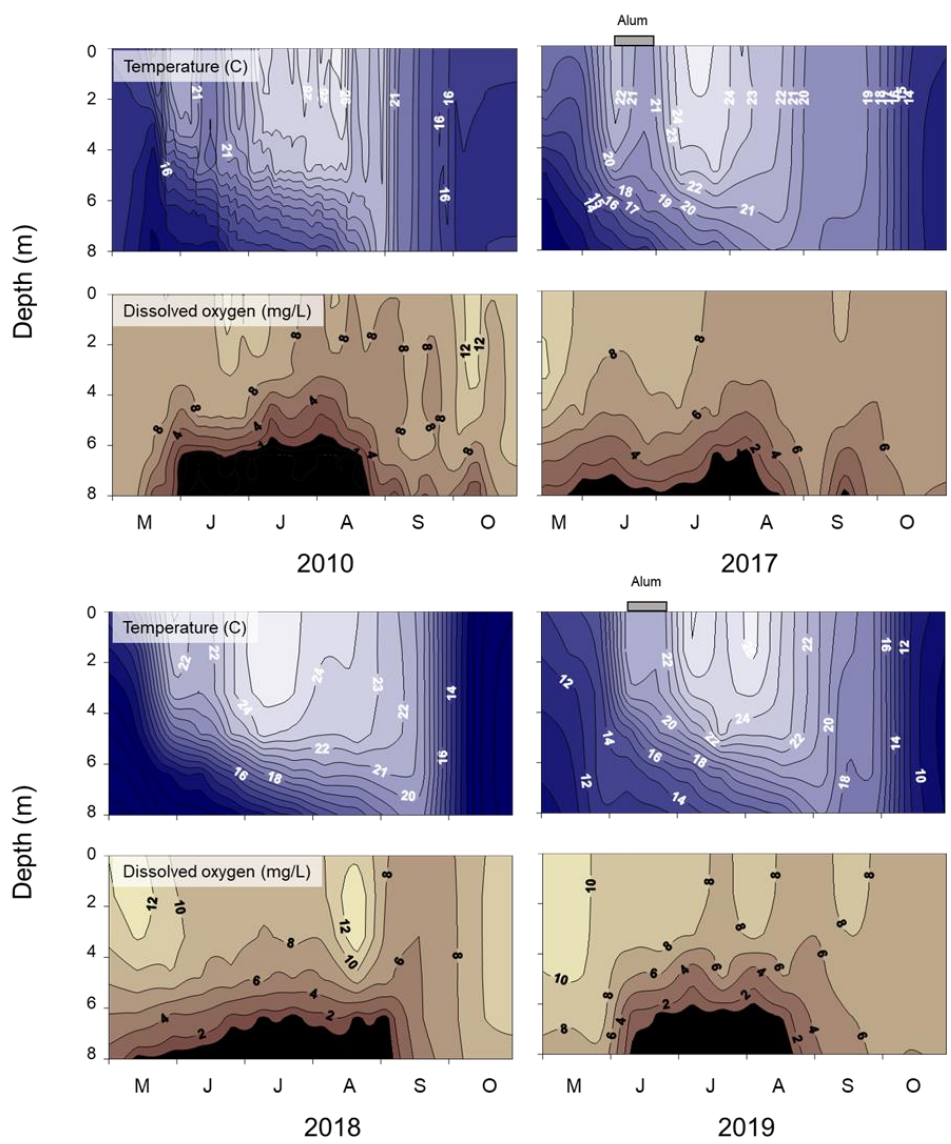


Figure 8. Seasonal and vertical variations in temperature (upper panels) and dissolved oxygen (lower panels) in 2010 (pre-treatment) and 2017-2019 (after alum treatment). Alum was applied in June 2017 and June 2019.

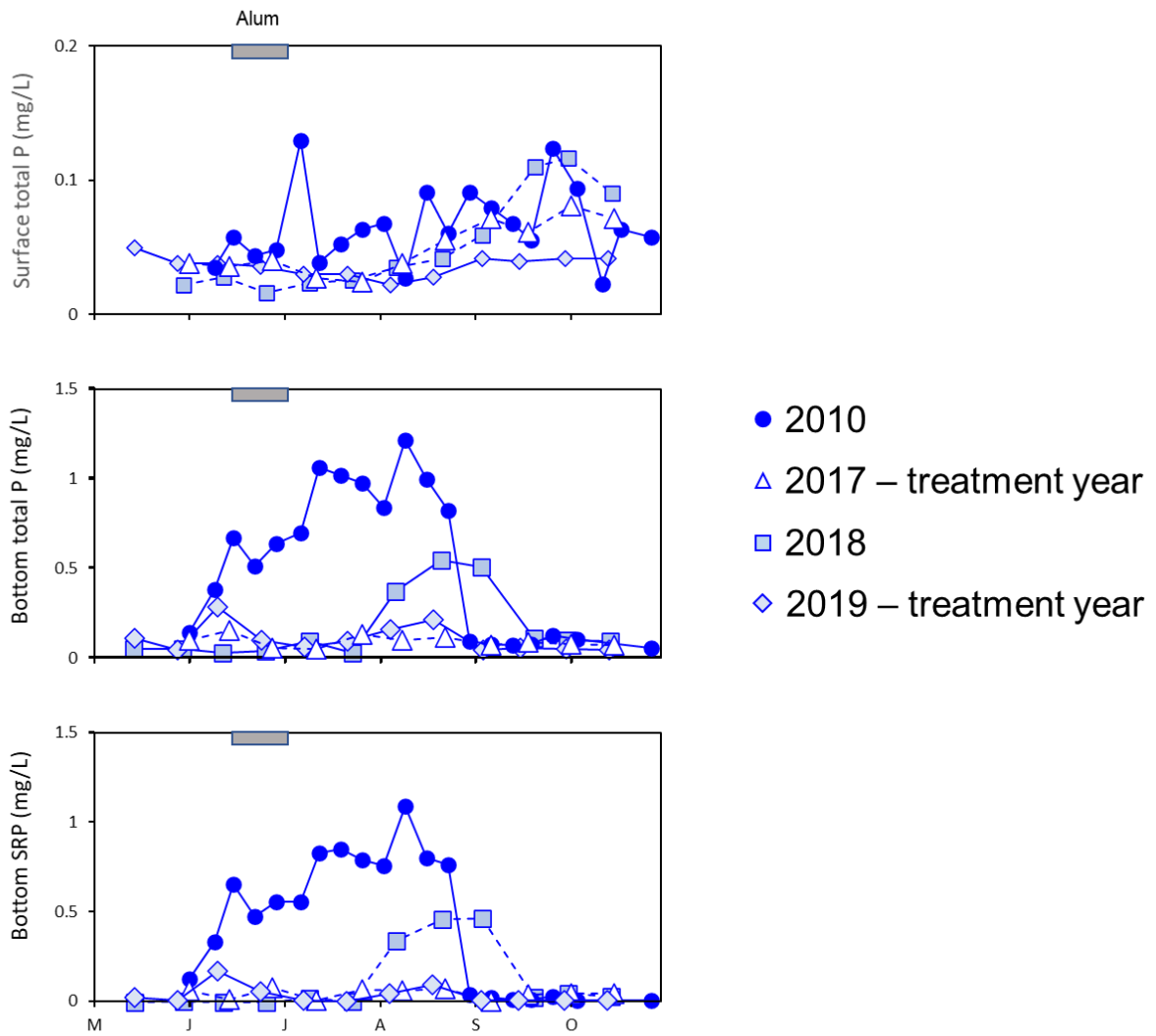


Figure 9. Seasonal variations in surface total phosphorus (P), bottom (i.e., ~ 0.25 m above the sediment-water interface) total P, and bottom soluble reactive P (SRP) during a pretreatment year (2010) and the post-alum treatment years 2017-19. Alum was applied in June 2017 and June 2019.

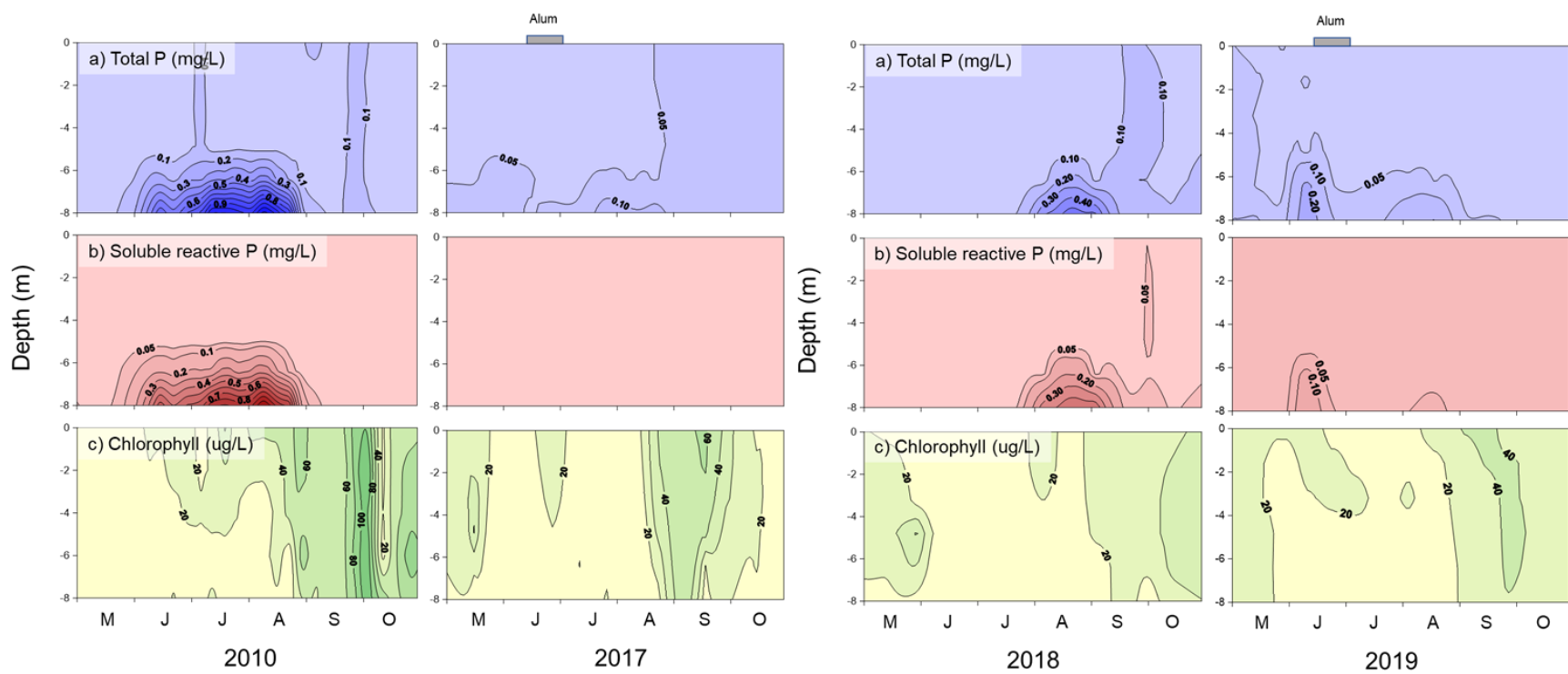


Figure 10. Seasonal and vertical variations in a) total phosphorus (P), b) soluble reactive P, and c) chlorophyll in 2010 (pretreatment) versus 2017-19 (post-treatment). Alum was applied in June 2017 and June 2019.

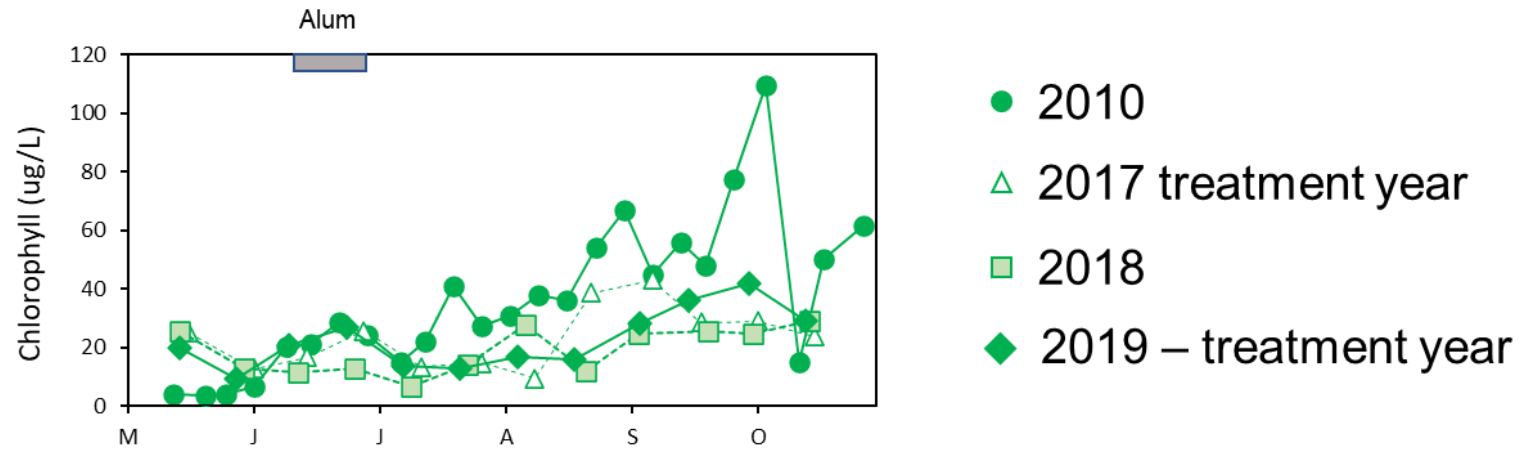


Figure 11. Seasonal variations in surface chlorophyll during a pretreatment year (2010) and the post-alum treatment years 2017-19. Alum was applied in June 2017 and June 2019.

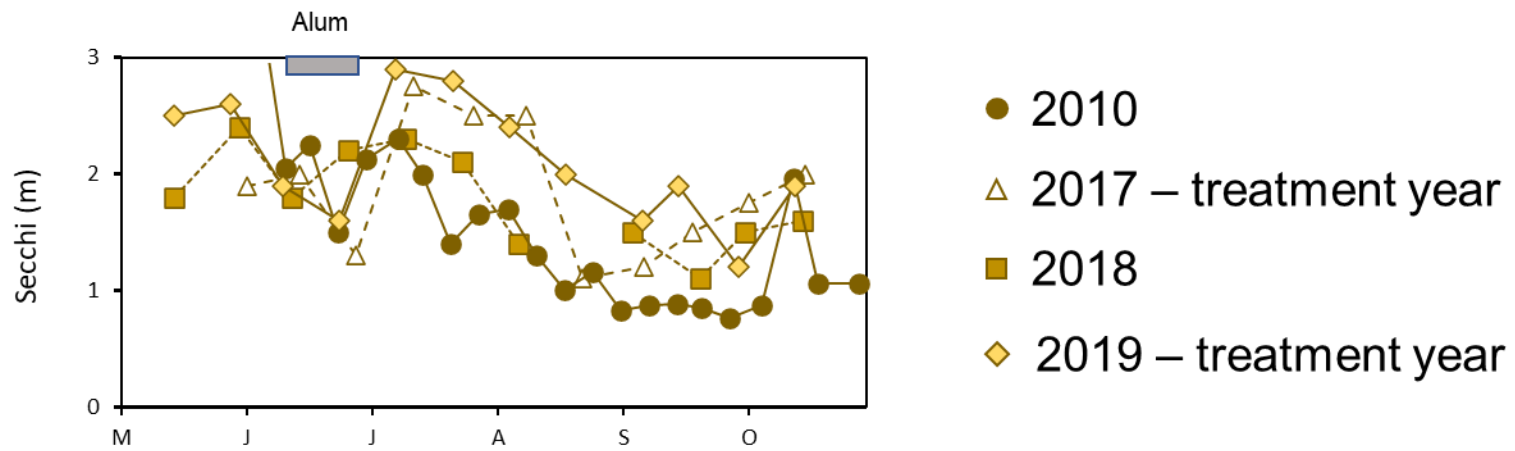
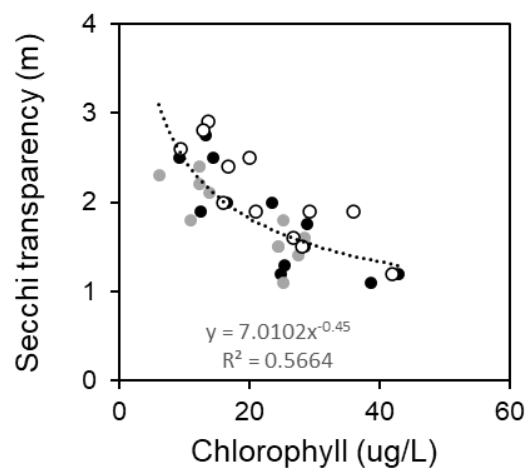
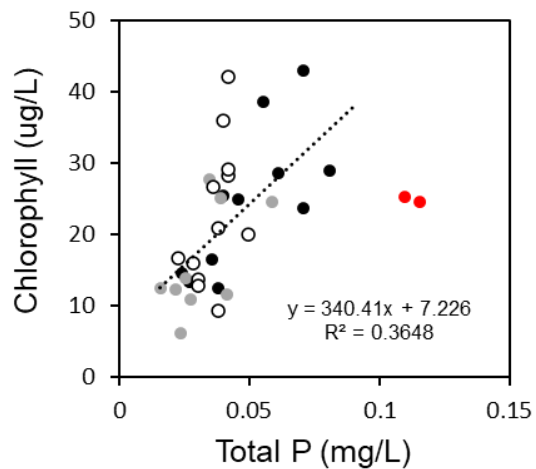


Figure 12. Seasonal variations in Secchi transparency during a pretreatment year (2010) and the post-alum treatment years 2017-19. Alum was applied in June 2017 and June 2019.

Figure 13. Relationships between Secchi transparency and chlorophyll (upper panel) and total phosphorus (P) versus chlorophyll (lower panel) during the summer 2017-2019.



- 2017
- 2018
- 2018 - outliers
- 2019



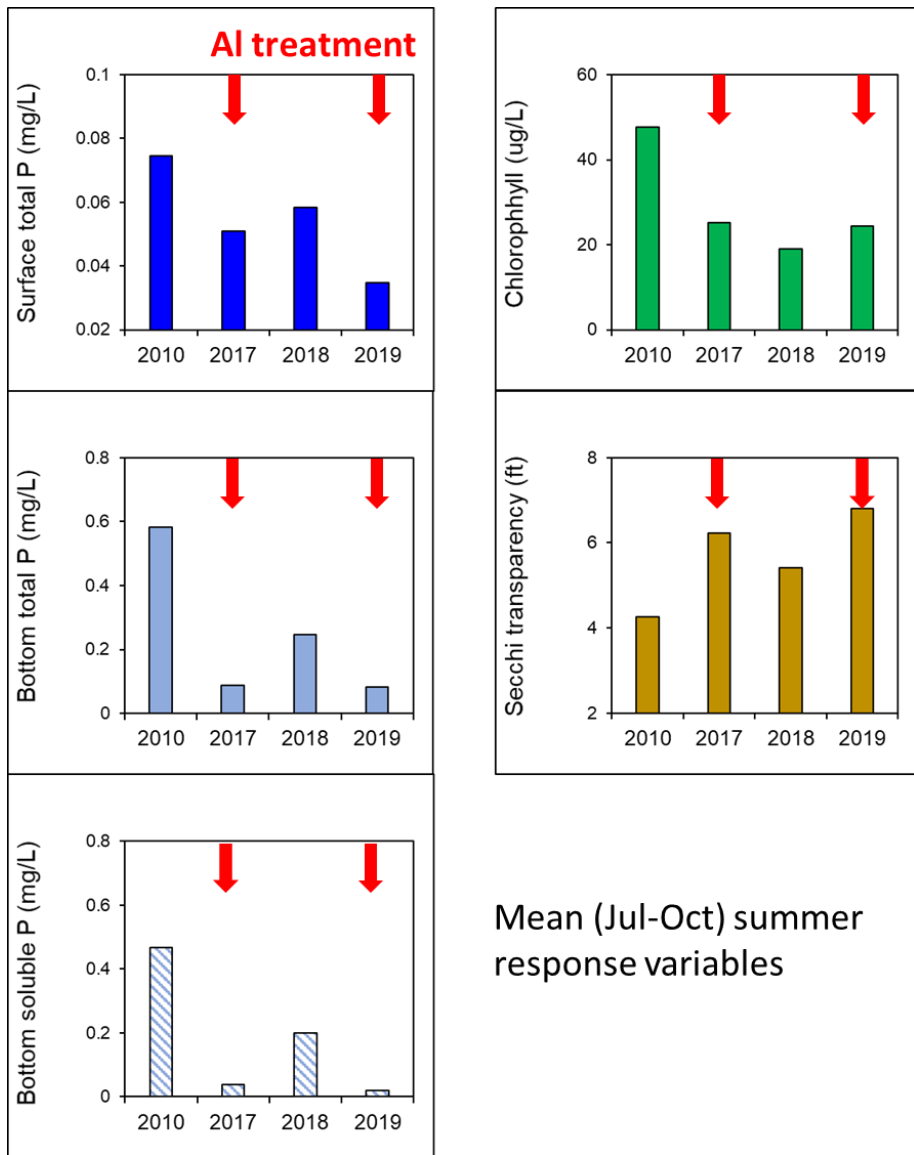


Figure 14. A comparison of mean summer (July-early October) summer concentrations of surface and bottom total phosphorus (P) and soluble reactive P (SRP), chlorophyll and Secchi transparency during a pretreatment year (2010) and the post-treatment years 2017-19. Alum was applied in June 2017 and June 2019.

Mean (Jul-Oct) summer response variables

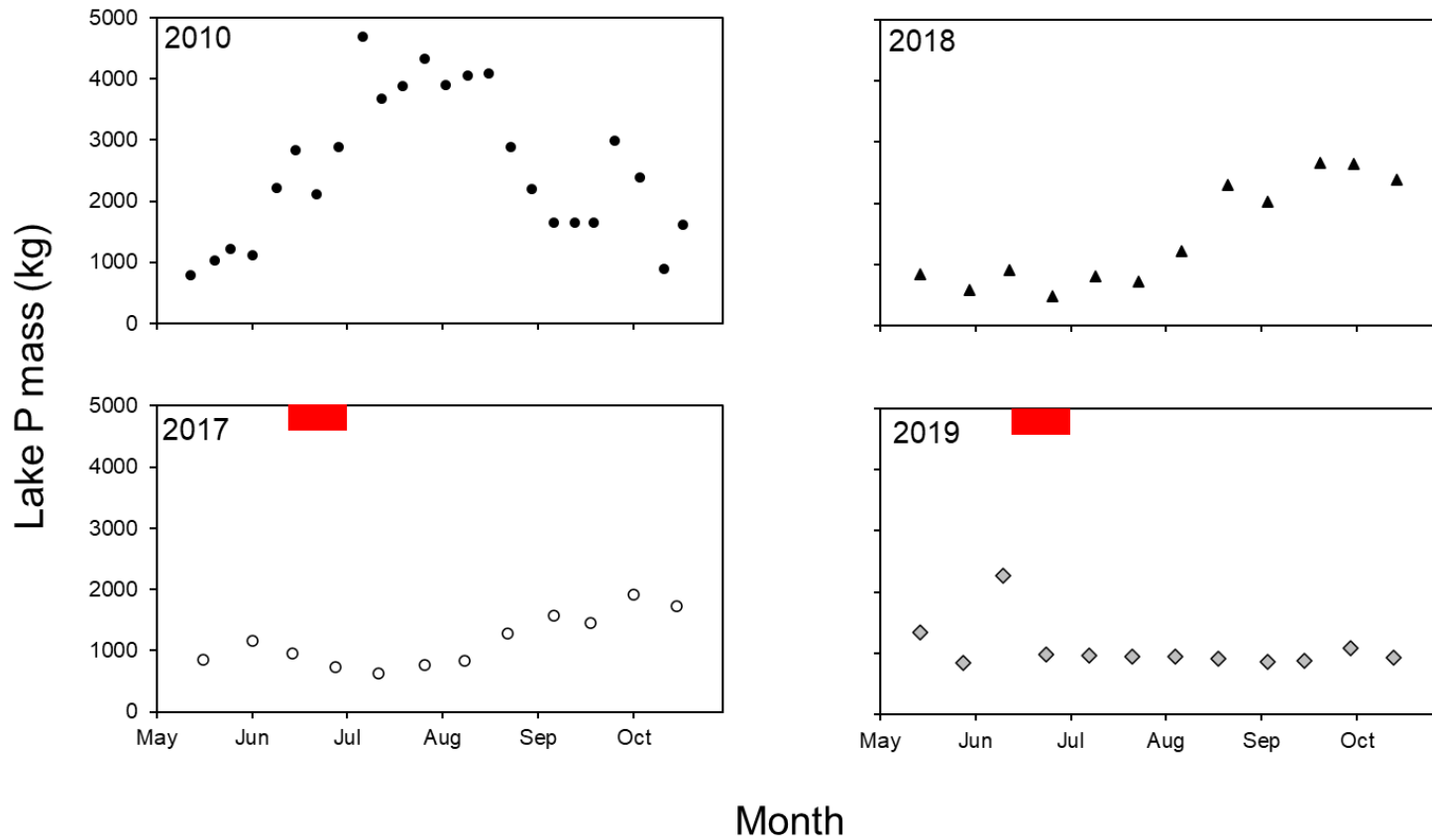


Figure 15. Seasonal variations in total phosphorus (P) mass during a pretreatment year (2010) and the post-treatment years 2017-19. Alum was applied in June 2017 and June 2019.

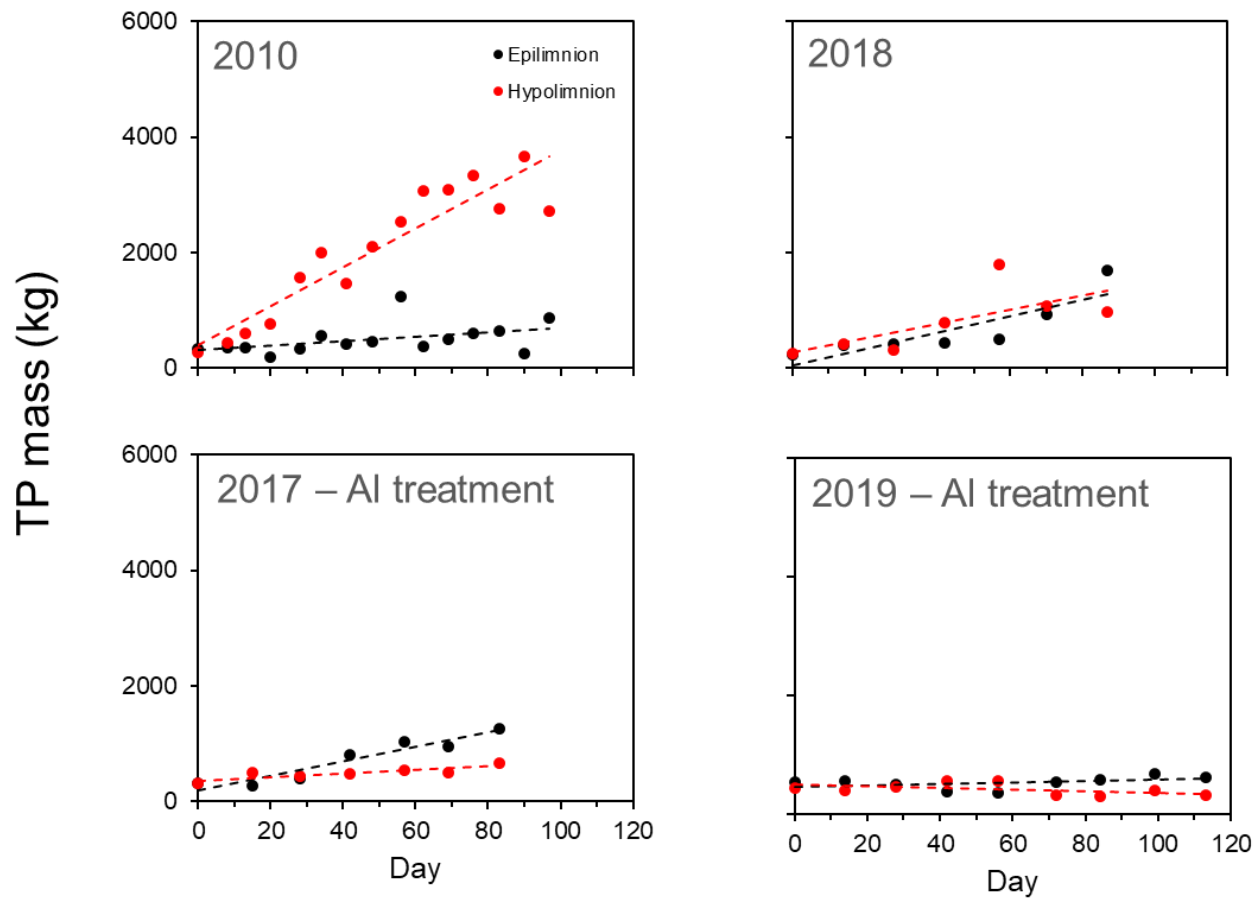


Figure 16. Seasonal variations in total phosphorus (P) mass in the epilimnion (i.e., 0-4 m) and hypolimnion (> 4 m) during a pretreatment year (2010) and the post-treatment years 2017-19. Alum was applied in June 2017 and June 2019.

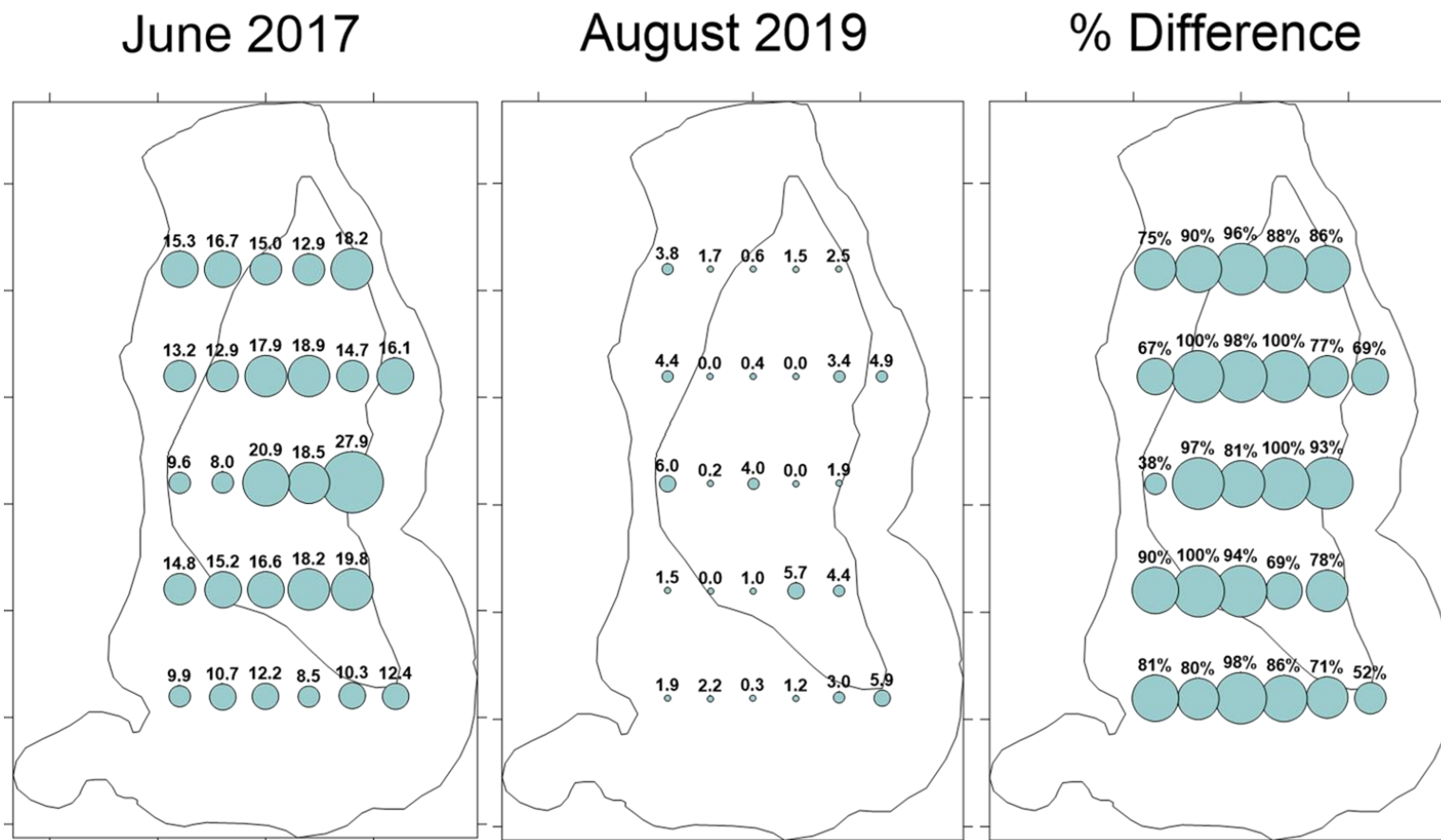


Figure 17. Spatial variations in anaerobic diffusive phosphorus (P) flux ( $\text{mg}/\text{m}^2 \text{ d}$ ) before (June 2017) and after (August 2019) the second alum application and the percent reduction (+) or increase (-) in the anaerobic diffusive P flux.

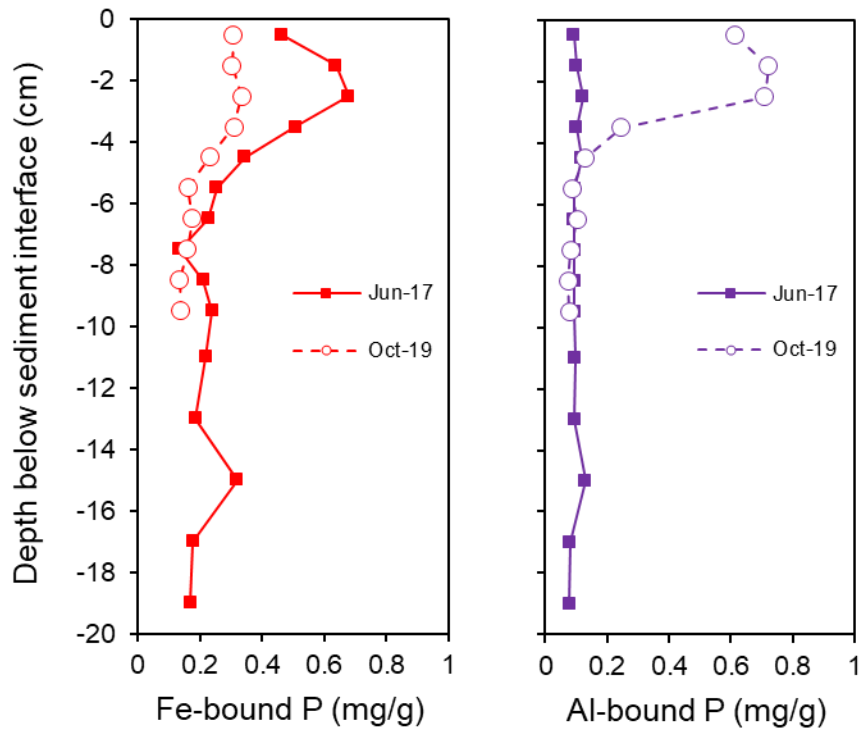


Figure 18. Vertical variations in sediment redox (i.e., the sum of the loosely-bound P and iron-bound P sediment fractions) phosphorus (P) and aluminum (Al)-bound P concentrations for a sediment core collected from station 2 (Figure 1) in June 2017 and August 2019. The sediment profile in June of 2017 represents pre-treatment conditions while August 2019 represents post-alum treatment conditions after two alum applications (2017 and 2019).